

## A Solid Target for SINQ based on a Pb-Shot Pebble-bed

F. Atchison and G. Heidenreich  
PAUL SCHERRER INSTITUTE  
CH-5232 Villigen PSI, Switzerland

### ABSTRACT

Preliminary results from scoping calculations examining the possibilities of implementing a Pebble-bed of Pb-shot as a target for SINQ are presented. The primary design objects are set out and estimates of heating and activation given. Cooling circuit parameters are discussed and estimates for operating conditions presented. A short discussion of problems associated with a realisation is included.

## 1 Introduction

Neutronic calculations [1] indicate a Pb-shot pebble-bed target system is capable of producing thermal fluxes at least as high as with the current engineered design for the liquid Pb-Bi eutectic mixture target. A solid-Pb target system has a less hazardous nuclide inventory and the activation locked in a solid matrix. It is also subject to less severe material compatibility difficulties (which in the case of the Pb-Bi target bring the majority of the flux loss). This opens the way to the production of a target system with large operational safety margins while using materials with 'neutronically' acceptable characteristics.

The prime requirement for the design is to maintain the integrity of the beam-window and to hold the Pb under its melting point. The major consideration is proton beam current density. The peak current-density at the design current of 1.5 mA and for all the beam passing through the up-stream meson target (Target-E) is predicted to be  $25 \mu\text{A}/\text{cm}^2$ . Any beam which by-passes Target-E will produce a smaller spot at SINQ. Such a beam condition is likely to arise from operational tolerances for the accelerator/proton-beam complex and may result in current densities up to  $100 \mu\text{A}/\text{cm}^2$  and for long periods; under extreme (and rare) fault conditions, the by-pass component could contain the whole beam and then the current density would reach  $260 \mu\text{A}/\text{cm}^2$ .

A target system unable to stand such high current densities would require protection systems against them. If the maximum handleable current density is too low, it will cause, at the minimum, a loss of thermal-neutron fluence from excessive beam interruptions. A reasonable margin of error is required: it should allow any remedial action to keep the beam matched to Target-E to be taken at a realistic speed, but has to be limited because of the technical difficulties of handling the high-power densities.

We take as primary specification that the target/beam-window system will be capable of normal operation (satisfies thermal and mechanical criteria) with a peak current density of  $100 \mu\text{A}/\text{cm}^2$  and, to limit the scope of accident-scenario discussion, will 'survive' current densities of  $260 \mu\text{A}/\text{cm}^2$ , for a short time period at least (it will have only marginal safety tolerances). Implicit in this specification is that the average peak current density over (say) one operational year remains close to  $25 \mu\text{A}/\text{cm}^2$ , i.e. a hundred or so hours at the higher current levels accumulated over the year.

The final design of the Pebble-bed target is to fit into the present geometry of the Pb-Bi version [2]. The neutronicly important region will be inside a cylinder of roughly 20 cm diameter and 100 cm long. This suggests an axial water flow as space limitations would make transverse cooling difficult to implement. On simplicity grounds, we consider a randomly packed bed and with the Pb-shot constrained into several sub-packets. At this stage we also restrict the considerations to the (most important) length of 50 cm which covers the main heating region. A sketch of the target is shown in Fig. 1.

Preliminary estimates for heating will be given in the next section and in the following two sections, cooling system parameters for the Pb-shot and the window respectively will be discussed. Section 5 will present activation estimates and a brief review of other considerations to be incorporated into a practical target design will be given in section 6.

## 2 Preliminary Estimates for Heating

A sketch of the target and moderator systems used for the neutronic estimates may be seen in Fig. 1 & 6 of [1]. Both activation (Section 5) and energy-density will vary somewhat with details of the design (maybe at the 10's of percent level) and will need recalculation when a detailed design for the whole system is available. Furthermore, the calculations have been made using a theoretical estimate for the proton beam distribution which corresponds to 'perfect matching' with Target-E (i.e. a peak current density of  $25 \mu\text{A}/\text{cm}^2$  at 1.5 mA). The energy balance for the inner part of the SINQ system with the Pb-shot target and for 570 MeV protons may be seen in Table IV of [1].

The pebble-bed has been represented in the calculation by a homogeneous mixture of 50% by volume Pb and  $D_2O$ . A simple hand estimate indicates that about 90% of the energy will be deposited in the Pb: an initial power density distribution for the Pb is based on the assumption that it receives all except the gamma-contribution (prompt nuclear and  $\pi^0$ ). The resulting power-density distribution is shown as a contour plot in Fig. 2.

For a beam current of 1 mA, the calculation gives the following values:-

	Total Power (kW)	Average Power Density (W/g)	Peak Power Density W/g
$D_2O$ (Direct)	33	-	-
Pb-Shot	385	6.7	37
Inner Al Wall	4.2	1.4	2.7
Outer Al Wall	4.4	1.2	2.4

The power-density for the window aluminium is given in terms of two factors: a conversion from proton beam current density at the window to power-density ( $2.5 \text{ W/g}$  for  $1 \mu\text{A}/\text{cm}^2$

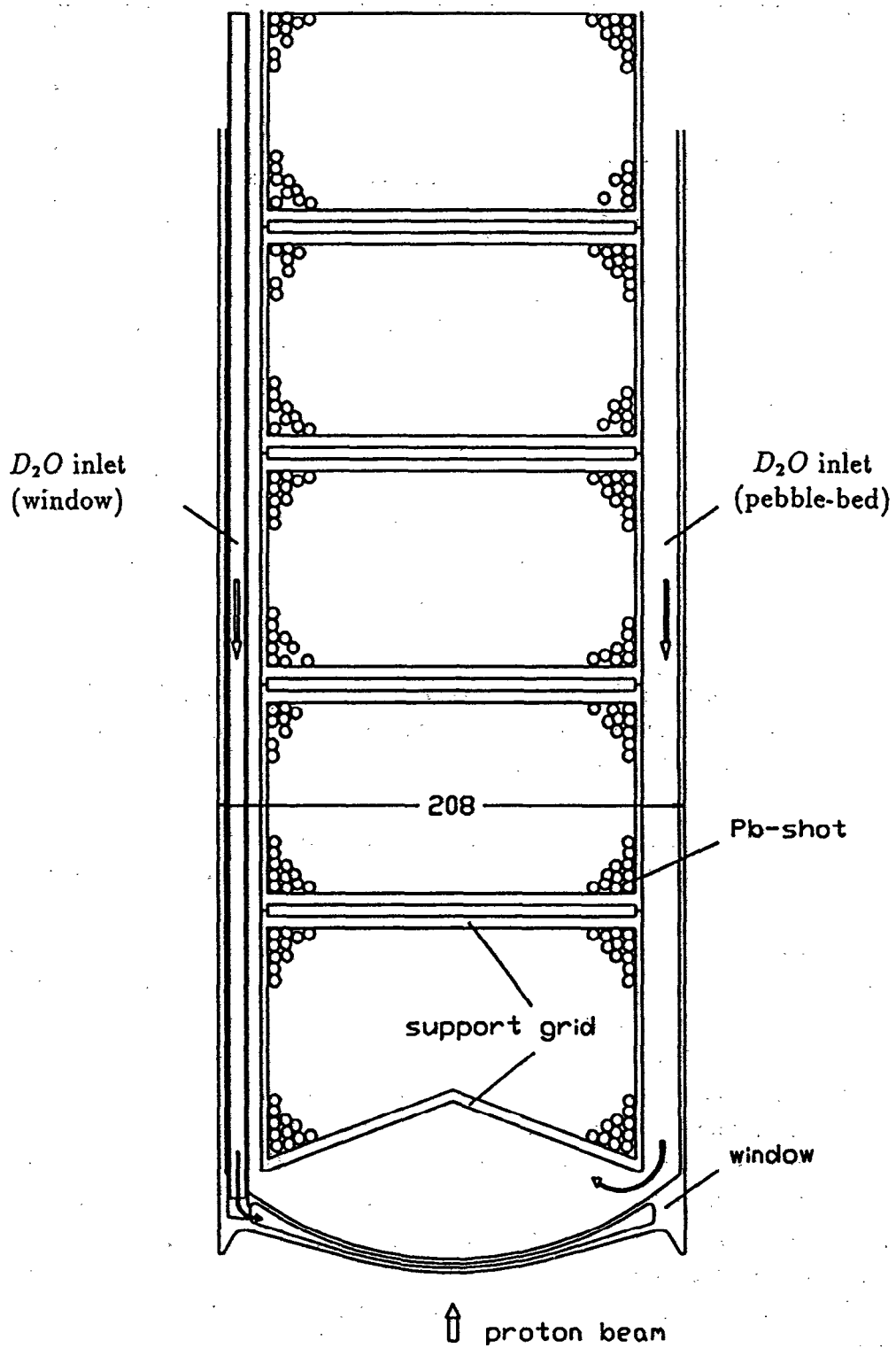


Figure 1: A sketch of the Pb Pebble-bed target. Aluminium is to be used for the material of construction and  $D_2O$  as the coolant for both the pebble-bed and the beam window.

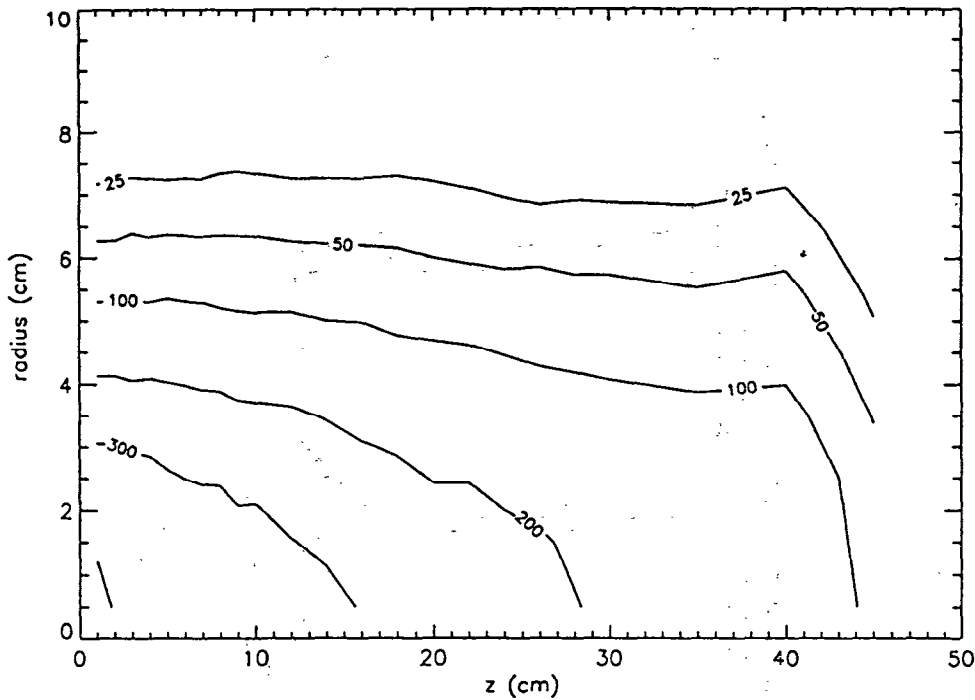


Figure 2: A contour plot of the power density distribution  $q_0(r, z)$ ,  $W/cm^3$ , in the Pb of the pebble-bed for a total current  $I_0$  of 1 mA,  $\sigma_0 = 4.36$  cm and a void fraction  $\phi_0 = 0.5$ .

proton beam current density) and a background contribution of 1.4 W/g/mA from neutrons, gammas etc. backscattered from the target which is approximately uniform over the whole surface of the window.

The critical regions from the cooling point of view are the beam-window and the pebble-bed. The basic results from the neutronic calculation need some processing so that they can be applied to the varying beam-size. The power density distribution in the pebbles depends on both the proton beam density and the void fraction  $\phi$  of the packed bed. The beam density distribution is approximated by a two component gaussian: one component represents the normal operation mode, where all the beam passes through the upstream meson target (Target E) and gives a standard deviation of  $\sigma_o = 43.6mm$ ; the second component represents a part  $\epsilon$  of the beam, which by-passes Target E and gives a standard deviation of  $\sigma_\epsilon = 13.4mm$ . Fig. 2 shows the power density distribution  $q_o(r_o, z_o)$  for a beam current  $I_o = 1mA$ , the standard deviation  $\sigma_o$  and a void fraction  $\phi_0 = 0.5$  of the packed bed. The values of  $q_o(r_o, z_o)$  has been scaled by the relations below, to calculate the power density distribution  $q(r, z)$  for the design current  $I = 1.5mA$ , the void fraction  $\phi = 0.4$  of a randomly packed bed and for a part  $\epsilon$  of the beam by-passing Target E.

$$q(r, z) = \frac{I}{I_o} \left[ (1 - \epsilon) + \epsilon \frac{\sigma_o^2}{\sigma_\epsilon^2} \right] q_o(r_o, z_o)$$

$$\text{where: } z_o = \frac{1 - \phi}{1 - \phi_o} z \quad \text{and} \quad r_o = \frac{\sigma_o}{\sigma_\epsilon} r$$

### 3 Cooling of the Pebble-bed

The parameters of the cooling system of the bed should satisfy the following general conditions:

- The maximum centre temperature of the Pb-shot should be below the melting point of Pb (327 °C) at incident proton beam current densities up to 100  $\mu\text{A}/\text{cm}^2$  and also for at least some time at 260  $\mu\text{A}/\text{cm}^2$  (we imply by this that at the highest power density safety margins will be very small - it is considered to be an extreme fault condition).
- The surface temperature of the balls should be below  $T_{sat}$ , the saturation temperature (Note: the high pressure loss means that  $T_{sat}$  will vary along the length of the pebble bed).
- A practical beam window to withstand the high current densities specified will not be able to stand pressures above about 12 bars.

There will be a range of operating conditions and so, following some introductory general considerations on power distribution, heat-transfer and pressure-loss in the pebble-bed, the ranges of these parameters will be considered in terms of a water-velocity - shot-diameter search space.

#### 3.1 Heat Transfer and Pressure Loss in the Packed Bed

The heat transfer coefficients,  $h$ , on the pebble surface are calculated from [3]:

$$h = Nu k_{fl} \frac{(1 - \phi)}{\phi d}$$

$$Nu = (0.4 Re^{0.5} + 0.2 Re^{0.67}) Pr^{0.4}$$

$$Re = \frac{v_z d}{\nu_{fl}(1 - \phi)}$$

where  $\nu_{fl}$  is the kinematic viscosity and  $k_{fl}$  the thermal conductivity of the coolant.

The pressure loss  $dP/dz$  in the bed is calculated using [4]:

$$\frac{dP}{dz} = \Psi \frac{\rho_{fl} v_z^2}{2d} \frac{1 - \phi}{\phi^3}$$

$$\Psi = \frac{320}{Re} + \frac{20}{Re^{0.4}} + 1.75$$

and where  $\rho_{fl}$  is the density of the fluid.

In Fig. 3 the pressure loss is presented as a function of the fluid velocity  $v_z$  measured in the empty bed and the pebble-diameter  $d$  for a void fraction  $\phi = 0.4$ . To avoid excessive stresses at the window, the pressure loss should not exceed  $\sim 12$  bar/m, which corresponds to an entrance pressure of 12 bars and an exit pressure of 6 bars for the 50 cm long bed.

### 3.2 Temperature Distribution

In the present axisymmetric model the temperature distribution of the fluid  $T_{fl}(r, z)$  within the packed bed is calculated by [5]:

$$\rho_{fl} c_{fl} v_z \frac{\partial T_{fl}}{\partial z} = k_r \left( \frac{1}{r} \frac{\partial T_{fl}}{\partial r} + \frac{\partial^2 T_{fl}}{\partial r^2} \right) + q_{fl}$$

where  $k_r = \rho_{fl} c_{fl} v_z \frac{F}{K} d$  represents the radial convective heat transfer,  $F$  is a shape factor ( $F=1.15$  for spheres) and  $K$  is a function of both the pebble and bed diameter ( $K=8.5$ );  $q_{fl} = q(1 - \phi)$  is the power density (normalized to the total volume) and  $c_{fl}$  is the specific heat of the fluid.

The surface temperature  $T_s(r, z)$  and the centre temperature  $T_c(r, z)$  of each spherical pebble are derived from:

$$T_s = q \frac{d}{6h} + T_{fl} \quad \text{and} \quad T_c = q \frac{d^2}{24k} + T_s$$

where  $k$  is the thermal conductivity of the solid lead.

The above formulism has been used to calculate the temperature maxima within the bed, normalized to the peak current density and as a function of the pebble-diameter and the fluid velocity. The results are presented in Fig. 4 for the  $D_2O$  temperature, Fig. 5 for the shot surface temperature and Fig. 6 for the centre temperature.

### 3.3 Operating Parameters

The results of the parameter survey (Figures 3 to 6) together with the constraints, allow construction of a velocity - diameter diagram describing the range where practical operating conditions exist. It will also indicate the process causing any limitation.

Taking 12 bars as the highest water pressure at the window, a pressure drop of 12 bar/m is a reasonable practical limit. This gives saturation temperatures of 190 °C at the window and 160 °C after 50 cm. As the contours indicate only the maximum values and not their position, we take 160 °C as the saturation temperature. Taking a water temperature of 40 °C at the start of the bed then the reduced temperatures at 25, 100 and 260  $\mu A/cm^2$  are:-

	25 $\mu A/cm^2$	100 $\mu A/cm^2$	260 $\mu A/cm^2$
$D_2O$ Temperature	4.8	1.3	0.46
Shot Surface Temperature	5.2	1.2	0.5
Shot Centre Temperature	11	2.9	1.1

These values are used to construct the velocity-diameter diagram shown in Fig. 7 for 100  $\mu A/cm^2$  and Fig. 8 for 260  $\mu A/cm^2$ . Any combination of values in the diagram (Fig. 7) are adequate for 25  $\mu A/cm^2$  and the range of choice to satisfy 100  $\mu A/cm^2$  is wide.

As the beam current density increases the working-space shrinks onto the '12 bar/m' line (see dashed lines in Fig. 7) indicating firstly the maximum current density handleable and secondly the optimum shot diameter: the values are about 170  $\mu A/cm^2$  and 5 mm shot diameter. The operational maximum will be at a somewhat lower current density to allow sufficient tolerance to handle the void fraction statistical variation from random packing. It

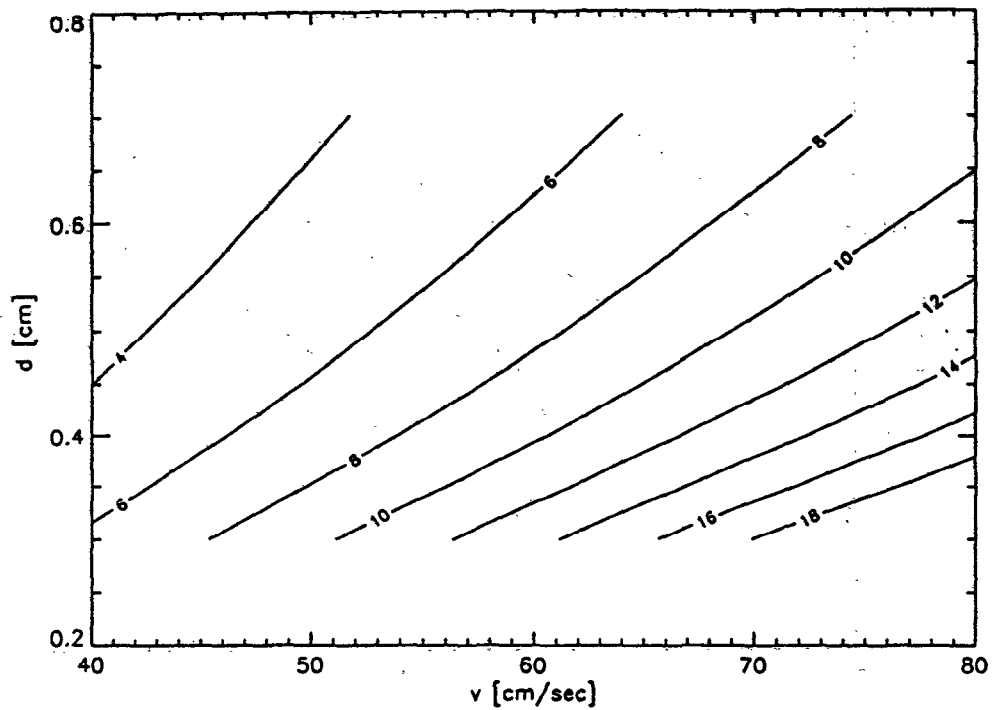


Figure 3: Contours of equal pressure loss (bar/m) as a function of water velocity and sphere diameter.

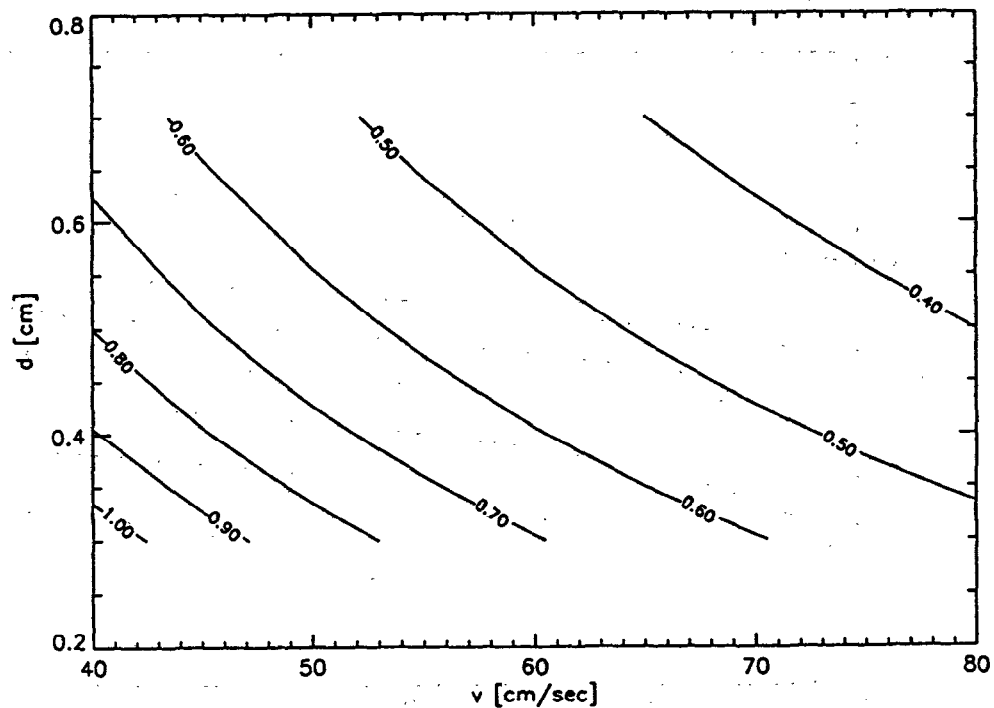


Figure 4: Contours of equal peak reduced  $D_2O$  temperature for a range of fluid velocities and Pb-sphere diameters. The reduced temperature is calculated from  $\frac{T_{fl} - T_{fl,in}}{\eta}$ , where  $\eta$  is the peak proton current density ( $\mu A/cm^2$ ),  $T_{fl}$  is the actual fluid temperature and  $T_{fl,in}$  is the temperature of the fluid at the start of the bed.

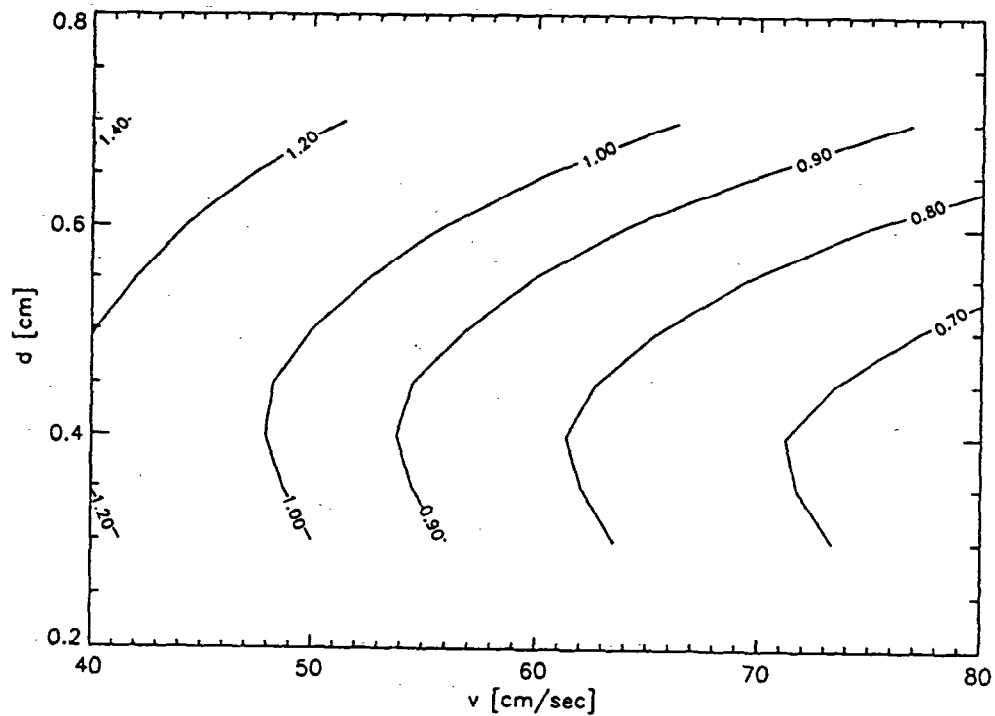


Figure 5: Contours of equal peak *reduced* Pb-sphere surface temperature for a range of fluid velocities and Pb-sphere diameters. The reduced temperature is calculated from  $\frac{T_s - T_{fl,in}}{\eta}$ , where  $\eta$  is the peak proton current density ( $\mu\text{A}/\text{cm}^2$ ),  $T_s$  is the actual surface temperature and  $T_{fl,in}$  is the temperature of the fluid at the start of the bed.

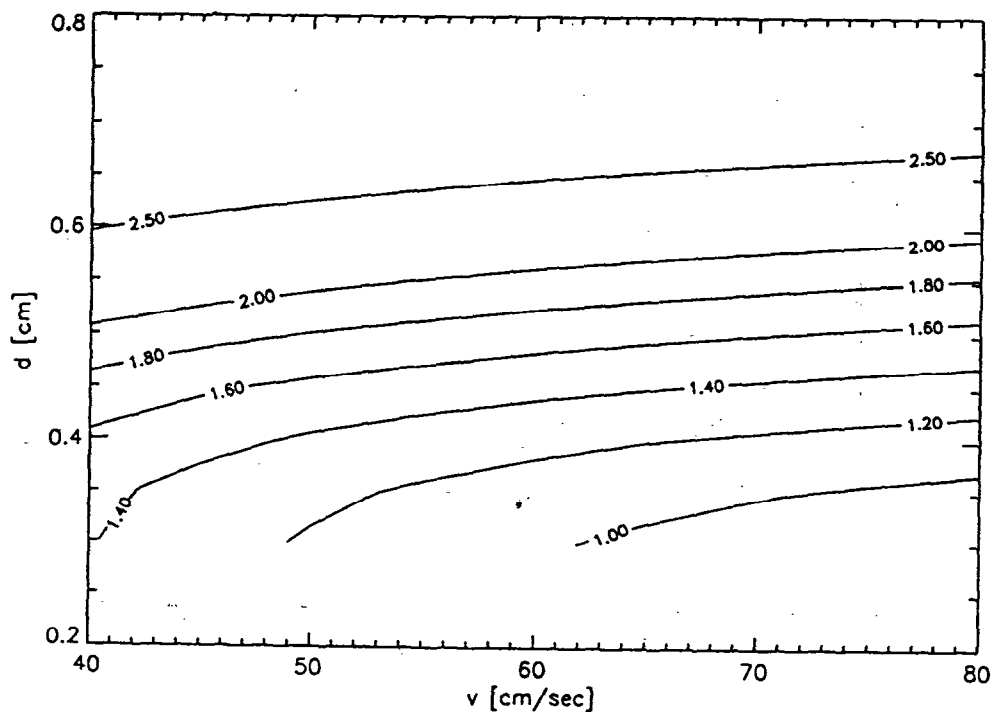


Figure 6: Contours of equal peak *reduced* Pb centre temperature for a range of fluid velocities and Pb-sphere diameters. The reduced temperature is calculated from  $\frac{T_c - T_{fl,in}}{\eta}$ , where  $\eta$  is the peak proton current density ( $\mu\text{A}/\text{cm}^2$ ),  $T_c$  is the actual peak centre temperature and  $T_{fl,in}$  is the temperature of the fluid at the start of the bed.



should also be noted that a higher maximum might be obtained if nucleate-boiling was included; this cannot be treated at this stage.

Fig. 9 shows a plot of the three pertinent temperatures ( $D_2O$ , surface and centre of the shot) along the axis of the bed for a current density of  $170 \mu A/cm^2$ , a shot of diameter 5 mm and a water-velocity of 75 cm/sec. Temperatures are well below their limiting values at all positions.

Fig. 8 shows that for a current density of  $260 \mu A/cm^2$  (Note: the higher velocity range), a simple 50 cm long pebble bed would require a pressure drop of 35 bar/m. This is considered to be incompatible with a practical beam window to handle the same current density.

The main limiting factor is the temperature of the  $D_2O$ . The lateral spread of the water flow through the pebble-bed is rather low. Consequently, too small a mass of water is available to handle the high power on the axis. The distribution of water temperature through the pebble-bed is shown as a contour plot in Fig. 10. This suggests that a fruitful approach would be to introduce 'flow-diverters' between the sections of the pebble-bed. These would laterally displace the axial water flow after some suitable distance down the pebble-bed and divert cooler water to the axis for the next section of the bed. The results of Fig. 9 & 10 would suggest a displacement of 1 or 2 cm after about 10 cm as being sufficient. No detailed work has been done on this yet.

## 4 Beam-Entry Window

The window has to pass 1.5 mA proton current with a peak current density that can reach  $260 \mu A/cm^2$ . There will be 12 bars static pressure on the inner side from the pebble-bed coolant and the proton-beam vacuum on the outer side.

The design for the outer (safety) element of the beam window for the Pb-Bi eutectic target [6] is taken as starting point. In this case, aluminium is to be the material of construction and (temperature dependent) material properties as for 6063 - T5 alloy have been used for the thermal and stress analysis made with the engineering analysis system ANSYS [7]. The window consists of two spherical caps with  $D_2O$  flowing between and is shown in Fig. 1. The aluminium thickness at the centre is 2 mm and the cooling will be supplied by an independent circuit. The power density distribution used has been described in Section 2. Heat transfer coefficients as for the earlier analysis [6] are used here:  $h = 2.6 W/cm^2/^\circ C$  for a flow velocity of 4 m/sec and a bulk temperature of  $40^\circ C$ . For the present, the cooling effect of the water for the pebble-bed is neglected so that for the present both elements are identical and cooled on one surface only. The extra cooling will improve the safety-factor of the inner element but the flow characteristics for the pebble-bed coolant in this region are not yet worked out.

The maximum temperature for the window at a peak current density of  $260 \mu A/cm^2$  is  $160^\circ C$  on the vacuum side. The von Mises stresses and the safety factor based on yield strength for peak current densities of 100 and  $260 \mu A/cm^2$  are given in the following table (the 50 mm radius roughly delimits the regions with and without beam heating):

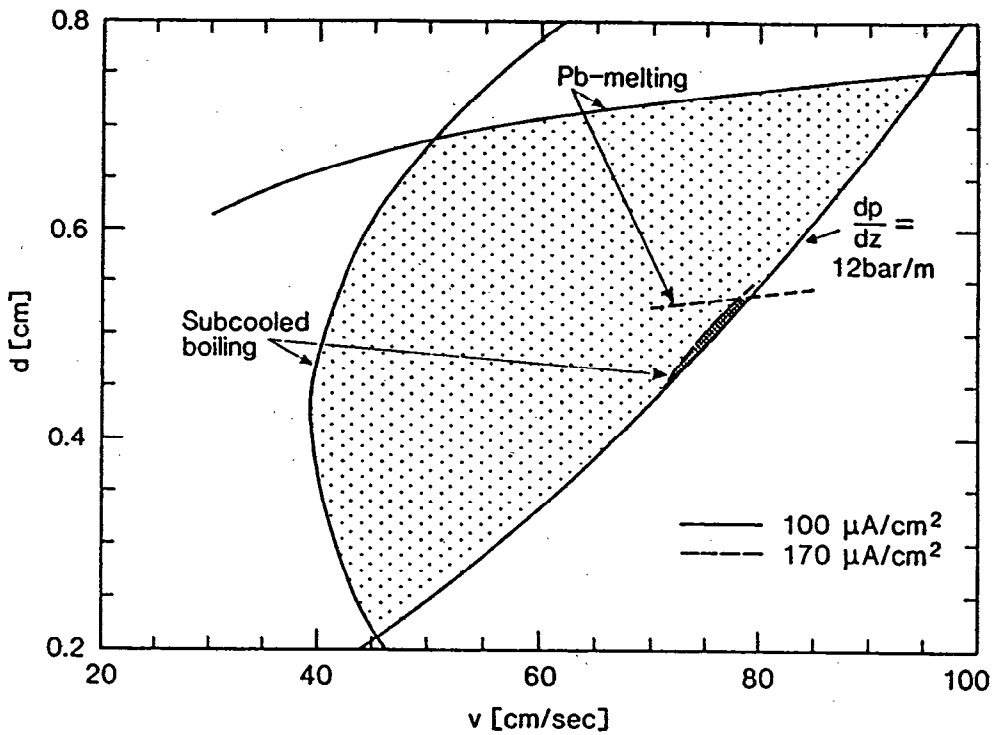


Figure 7: Operating region for velocity and shot diameter values in a simple random-packed (void fraction = 0.4) pebble-bed of length 50 cm at a beam current density of  $100 \mu\text{A}/\text{cm}^2$  and for a pressure of 12 bars on the window. The dashed lines show the operating region for  $170 \mu\text{A}/\text{cm}^2$  (roughly the maximum) and indicates an optimum shot diameter of 0.5 cm.

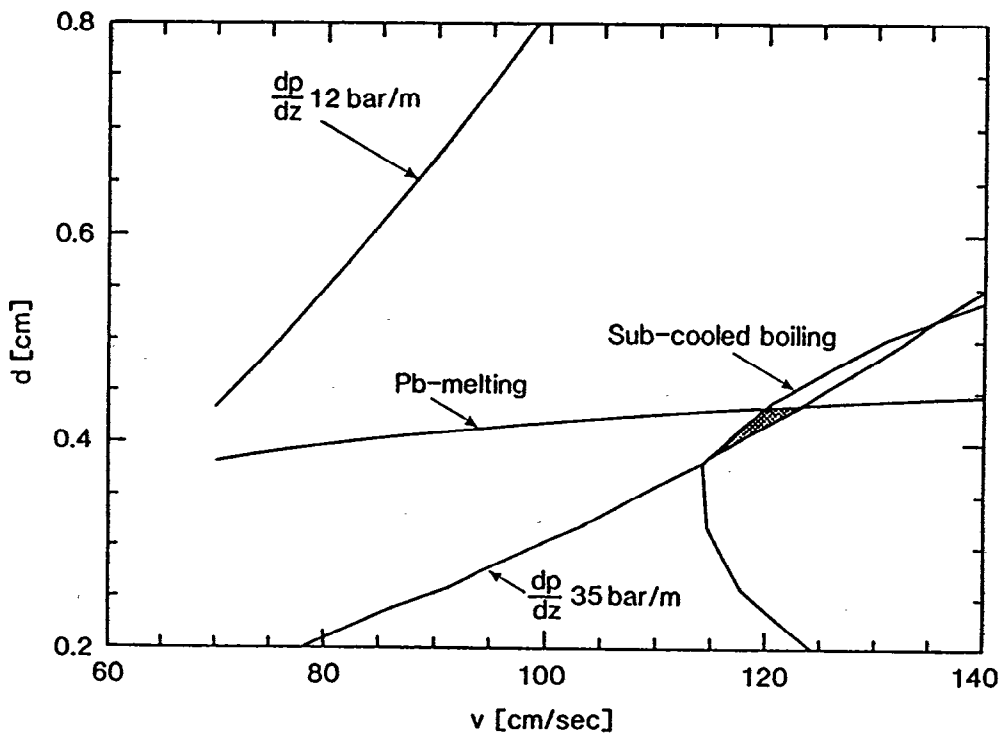


Figure 8: Operating region for velocity and shot-diameter values for  $260 \mu\text{A}/\text{cm}^2$  (Note the different velocity scale compared to Fig. 7).

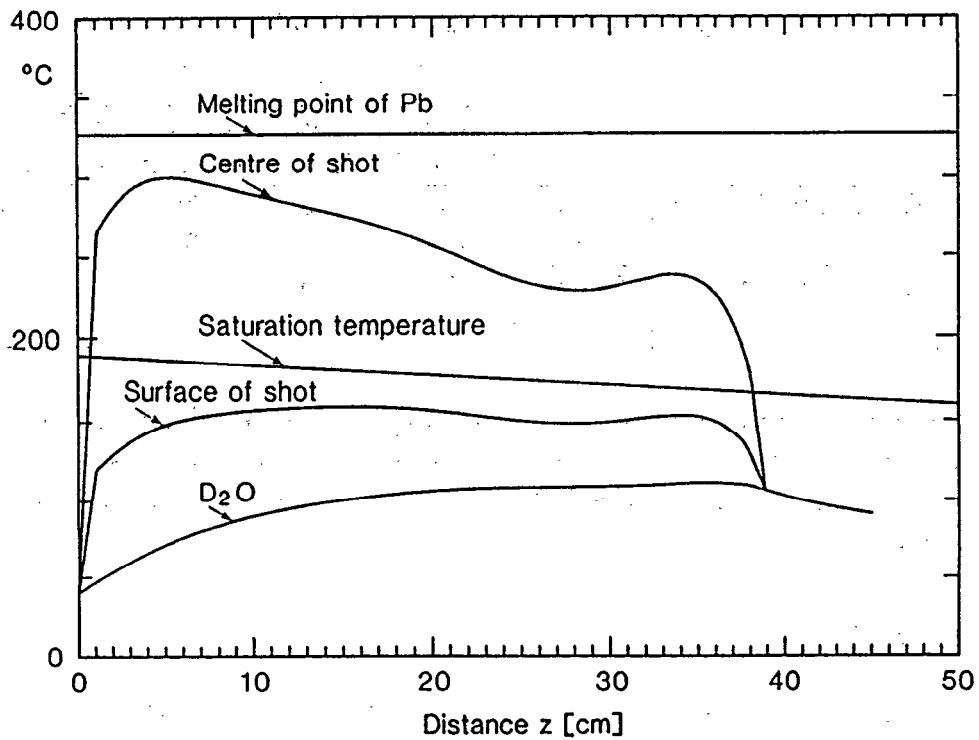


Figure 9: Axial temperature distribution at a peak current density on the beam window of  $170 \mu\text{A}/\text{cm}^2$  through a pebble-bed with 5 mm diameter Pb-shot and a  $D_2O$  velocity,  $v_z$ , of 75cm/sec. A water temperature of 40 °C at the start of the pebble-bed has been assumed.

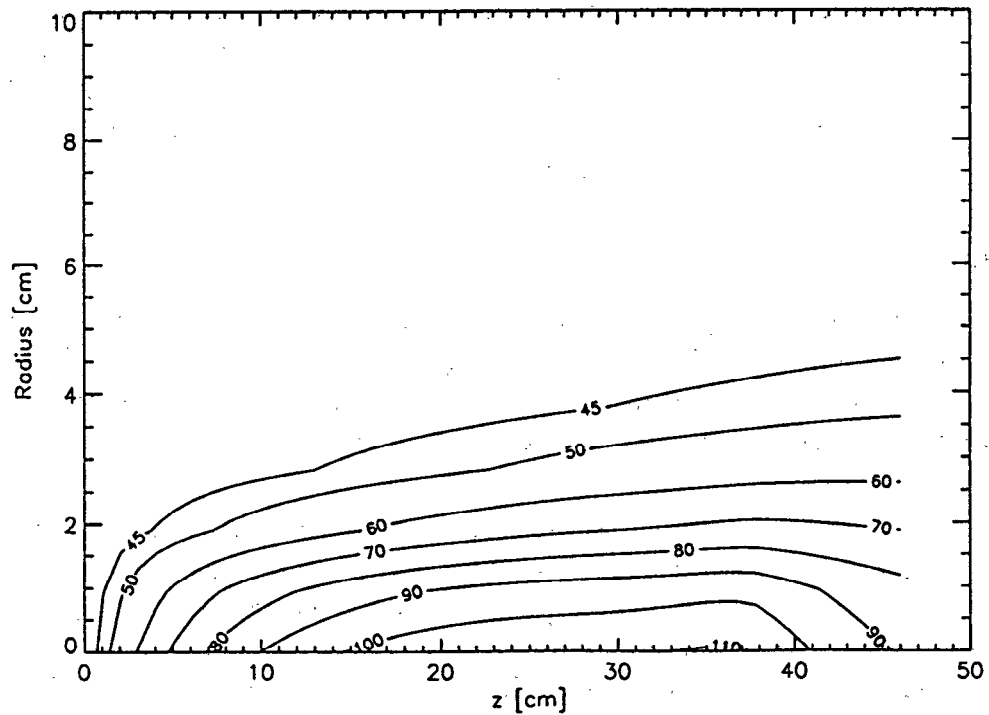


Figure 10: Contour plot of the fluid temperature in the pebble-bed as a function of depth ( $z$ ) and radius. The conditions are: water velocity = 75 cm/sec, sphere diameter 5 mm, proton beam current density =  $170 \mu\text{A}/\text{cm}^2$  and inlet water temperature 40 °C.

von Mises Stress and safety factor.  
( $p_{window} = 10$  bars,  $p_{pebble-bed} = 12$  bars)

		100 $\mu\text{A}/\text{cm}^2$		260 $\mu\text{A}/\text{cm}^2$	
		Stress N/mm <sup>2</sup>	Safety Factor	Stress N/mm <sup>2</sup>	Safety Factor
Outer Window	$r \leq 50$ mm	40	3.5	70	2
	$r \geq 50$ mm	139	1	137	1
Inner Window	$r \leq 50$ mm	43	3.5	125	1
	$r \geq 50$ mm	20	7	20	7

This indicates a window to pass 260  $\mu\text{A}/\text{cm}^2$  is practicable (the calculations are made with a minimally modified existing design). The main stress is caused by the static water pressure for the window coolant and the safety factor of 1 in the outer regions is indicative of the need for some design modifications.

## 5 Activation

A major consideration in the design is activation. A great practical advantage of the Pb-Bi target is that the main bulk of the total activation is sealed into a container and also the activation is diluted through a large mass of material. The activation of the Pb is less hazardous but the specific activation (and hence after-heat) will have a higher density and also the cooling  $D_2O$  is directly irradiated by the beam. Corrosion and the direct activation means that the external parts of the cooling circuit will have to incorporate adequate safety precautions.

The activation estimates come from the same calculation used for heating (see Section 2) and take into account nuclides produced by the high-energy particle cascade, fast and epithermal neutrons, thermal neutrons and (in the case of the Pb-shot) polonium production via  $\alpha$ -particle induced and double production processes. No direct estimate for tritium production in the high-energy cascade is available at this time.

### 5.1 Lead

The build-up of secondary-product mass, activation, 'burden'<sup>1</sup> and decay power for 1 mA operation is shown in Table-I (a) and the decay following 1 year in operation in Table-I (b). The lower value of both activity and decay heating compared to Pb-Bi comes from the removal of the Bi: the majority of the active isotopes of Bi and Po with their relatively high decay energy are eliminated.

The activation at one year corresponds to an average value of 4.7 Ci/g and the decay power to 18 mW/g. There will be a systematic variation of the nuclide inventory within the activated region, but approximate values for the peak values may be obtained using the power density distribution. These are 27 Ci/g and 100 mW/g. Some reduction of the peak decay power will come from the energy dispersion by the (about 80%) gamma contribution.

<sup>1</sup>This term has been coined internally within the SINQ project to give a measure of the activation in terms of its potential hazard - the activity is multiplied by the DECO (Dose Equivalent to Critical Organ) factor to give an effective dose in rems.

Table-I

(a) The build-up of mass, activation, 'burden' and decay-power as a function of irradiation time at a current of 1 mA.

Irradiation Time	Mass g	Activation kCi	'Burden' Mrem	Decay-Power Watts
10 d	2.56	236	426	948
100 d	25.3	259	734	1030
1 y	92.2	270	962	1060
2 y	185	277	1090	1080

(b) The decay of activation, 'burden' and total decay power as a function of time following one year in operation at 1 mA. Except for short decay times, just over 80% of the decay power is radiated as gammas.

Decay Time days	Activation kCi	Burden Mrem	Decay-Power Watts
0	270	962	1080
0.1	180	930	620
10	27	490	99
100	8.3	220	21
365	2.5	95	5.8

The 'burden' for the nuclide inventory is 962 Mrem after 1 year in operation at 1 mA. This is a factor of about 74 lower than with the Pb-Bi target. The major contributors (collected by element) together with the values for Pb-Bi, are shown in Table-II.

## 5.2 Aluminium Container

The specific equilibrium activation (averaged over a 45 cm length of the walls) for products with half-lives greater than 10 mins (the shorter half-life products contribute about 18 Ci/g) at a beam current of 1 mA are:-

Nuclide	Half-life	Decay Mode	Equil. Activity Ci/g
$^{24}\text{Na}$	15.0 h	$\beta^- \gamma$	0.029
$^{22}\text{Na}$	2.60 y	$\beta^+ \gamma$	0.046
$^{21}\text{Na}$	22.5 s	$\beta^+ \gamma$	0.0075
$^{18}\text{F}$	110 m	$\beta^+$	0.037
$^3\text{H}$	12.3 y	$\beta^-$	0.13

The contribution from Tritium has been estimated using the approximation (suggested by the value from Oxygen) that production corresponds to 10% of the high-energy cross-section. The activation of the aluminium is mainly of interest as a potential contribution to activity in the coolant from corrosion.

Table-II

The major contributors to 'burden' (Mrem) with the Pb target and the Pb-Bi targets after operation at 1 mA for 1 year.

Element	Pb-Target	Pb-Bi Target
I	134	305
Sr	100	149
Ir	94	3
Hg	75	47
Y	73	116
Pb	73	39
Bi	68	13900
Tl	62	72
Po	54	56200
Xe	38	68
Os	27	20
Pt	25	27
Cd	20	42
Yb	17	17
Ce	10	21
Others	92	174
Totals	962	71200

### 5.3 Heavy Water

The build-up of activation and specific activation at given locations will depend on the conditions of the circuit: for an irradiation volume  $V$  in which the coolant is irradiated for a time  $t_{irr}$ , a coolant circulation time of  $t_{circ}$  and a total time in operation  $T (= N \cdot t_{circ})$  and only relevant for long half-life products), the specific activation at the *end* of the irradiation volume is given by:-

$$I = \sum_i J_i = \sum_i \frac{\alpha_i}{V} \cdot \frac{(1 - \exp^{-\tau_i t_{irr}})(1 - \exp^{-\tau_i T})}{(1 - \exp^{-\tau_i t_{circ}})}$$

where  $\alpha_i$  is the equilibrium activation and  $\tau_i$  the decay constant for nuclide  $i$  (in the one or two cases where there is a decay chain, this expression needs an obvious modification to treat the daughters). The specific activation at some position with a time-delay from the end of the irradiation volume of  $t_{dec}$  is obtained by introducing the appropriate exponential factor into the sum over nuclides.

To give some feel for the orders of magnitude, Table-III shows values of the specific activation calculated with some 'guess' parameters (see the caption). The majority of the products are short-lived and will decay to negligible levels shortly after beam switch-off. The presence of  $^{17}N$  will be noted in the design of the plant: being a comparatively long half-life neutron emitter it has the potential to cause activation to some degree *throughout* the cooling circuit. The tritium activity will approach 2400 Ci (but only in times given by the build-up with a 12.3 year half-life: 120 Ci at 1 year; 980 Ci at 10 years; 1900 Ci at 30 years).

Table-III

Specific activation, Ci/litre, for the  $D_2O$  coolant by nuclide and using the circuit parameters: flow velocity 0.5 m/sec, irradiation volume 8.8 lit., irradiation time (per circulation) 1.8 sec. and a circulation time of 230 sec. (i) at the end of the irradiation volume,  $A_{irr}$ , (ii) at a point beyond the end of the irradiation volume reached in 50 seconds,  $A_{det}$ , (Note: only nuclides giving significant contribution at this point are included in the table) and (iii) the equilibrium specific activation,  $A_{eq}$ .

Nuclide	Half-life	Decay Mode	$A_{irr}$	$A_{det}$	$A_{eq}$
$^{15}O$	2.03 m	$\beta^+$	7.3	5.5	520
$^{14}O$	70.59 s	$\beta^+\gamma$	0.42	0.26	22
$^{17}N$	17.0 s	$\beta^-n^0$	0.017	0.023	2.5
$^{16}N$	7.13 s	$\beta^-\gamma$	8.7	0.067	54.0
$^{13}N$	9.96 m	$\beta^+$	0.95	0.90	110
$^{14}C$	5730 y	$\beta^-$	$2.3 \cdot 10^{-5}$	$2.3 \cdot 10^{-5}$	83
$^{11}C$	20.38 m	$\beta^+$	0.33	0.32	47
$^{10}C$	19.3 s	$\beta^+\gamma$	0.45	0.074	7.2
$^{13}B$	17.33 s	$\beta^-\gamma$	0.31	0.042	4.5
$^{11}Be$	13.8 s	$\beta^-\gamma$	0.035	0.0028	0.41
$^{10}Be$	$1.6 \cdot 10^6$ y	$\beta^-$	$1.9 \cdot 10^{-8}$	$1.9 \cdot 10^{-8}$	20
$^7Be$	53.29 d	EC	0.082	0.082	13
$^3H$	12.3 y	$\beta^-$	0.039	0.039	275
Totals			202	7.3	1340

### 5.4 Lead Corrosion

The  $D_2O$  coolant will be contaminated by corrosion/erosion products. The principal cause for concern is the Pb-shot which will present a large surface area to the coolant and also probably collide with one another giving an erosion contribution.

Although the exact process rates have not yet been established, order-of-magnitude estimates of the activation aspects are useful at this stage to see the potential extent of the problem: cladding of the shot is planned but the degree of quality control and the consequence of failure depend critically on the hazard being inhibited.

The build-up of activation in the  $D_2O$  will be non-linear. If the production rate, in the target, for a nuclide with decay constant  $\lambda$  is  $\dot{q}$  g-atom/sec, then, neglecting feeding from chains, the activity after some time  $t$  will be  $A$  given by:

$$A = 1.628 \cdot 10^{13} \times \dot{q} \times (1.0 - \exp^{-\lambda t})$$

If the target material enters the  $D_2O$  at a rate  $\dot{C}$ , then the build-up of the coolant activity will be:

$$\dot{C} \cdot A \cdot \frac{1}{\lambda} \cdot (1.0 - \exp^{-\lambda t}) = 1.628 \cdot 10^{13} \times \dot{q} \times \dot{C} \times \frac{1}{\lambda} \times (1.0 - \exp^{-\lambda t})^2$$

From this it may be seen that the short lived nuclides will reach an equilibrium of:

$$\frac{1}{\log_e 2} \times \dot{Q} \times t_{\frac{1}{2}} \times A$$

where  $\dot{Q}$  is the *fractional* rate of entry into the  $D_2O$  of the *mass of target material containing* the (equilibrium) activity  $A$  and the decay constant has been expressed in terms of the half-life in seconds. Expanding the exponential term, it may be seen that to first order, the long half-life nuclides will build-up according to a  $t^2$  law.

The target activity is spread over about 1000 nuclides and requires chain-yield analysis. A first approximate numerical solution to give a feel for the orders of magnitude has been obtained using 0.1 cm/year for  $\dot{Q}$  (we note that such a value is probably unacceptably high).

The activation build-up over a one-year period has been estimated by taking 10 equal time steps. The nuclide feed-rates into the  $D_2O$  are taken as constant over each time step using (i) a corrosion rate which is constant within the interval and (ii) values of the nuclide densities in the target at the middle of each period.

The build-up of the mass (Note: this is the mass of the products, NOT the mass corroded), activation and the 'burden' (see footnote above) in the  $D_2O$  for the three corrosion rates are shown in Table-IV (a) and the decay after a 1 year irradiation in Table-IV (b).

The estimated activation entering the  $D_2O$  is about 3 kCi (that is, about 1% of the activity in the target) and varies essentially linearly with total corrosion rate (i.e.  $\dot{Q}$ ). This is of the same order of magnitude as for the (short-lived) activation of the  $D_2O$  in operation and the tritium after long-term operation.

The contributing nuclides are biased toward 'nastier' medium-to-long half-life isotopes, as may be seen from the relatively slow decrease with time and also from the 'burden' (about 6% of that for the target or a factor of six higher per Ci as compared to that for the nuclide mix in the target).

The majority of the nuclides presumably will be caught in filters or resin-beds: these will need to be shielded. The gamma intensity (summed over all nuclides in the  $D_2O$ ) is about  $2.3 \pm 0.3 \cdot 10^{10}$   $\gamma$ /second/Ci with a mean energy of  $0.58 \pm 0.06$  MeV where the spread in values is systematic with cooling period (rather higher at short and very long times) due to the changes in the nuclide mix.

## 6 Summary and Further Design Considerations

In the previous sections we have shown that the essential parts of a Pb-shot pebble-bed target system (the beam-window and the cooling of the shot) will operate with proton current densities over  $100 \mu\text{A}/\text{cm}^2$ : i.e. the window has an engineering safety factor of greater than 3, the Pb-shot is well below the melting point everywhere and neutronicly acceptable materials are used. The window system should also withstand the extreme 'fault-condition' current density of  $260 \mu\text{A}/\text{cm}^2$  but, at the present stage of the study, we have not completed investigations for a system in which the Pb-shot will not melt at this highest current density.

Corrosion. The Pb-shot will present a large surface area (about  $6 \text{ m}^2$ ) to the  $D_2O$  and even a normal corrosion rate for the Pb-water system ( $0.005 \text{ cm}/\text{year}$ ) will lead to rather large quantities of Pb entering the coolant (about  $4 \text{ kg}/\text{year}$ ). The extra activation lodged in the external circuit would be about 300 Ci after one year's operation. A higher corrosion rate



Table-IV

(a) The mass, activity and 'burden' for nuclides entering the  $D_2O$  by corrosion for an average corrosion rate of 0.1 cm/year and a surface area of 3 m<sup>2</sup>.

Time y	Mass g	Activity Ci	'burden' Mrem
0.1	0.282	683	6.5
0.2	1.09	1050	14
0.3	2.39	1350	21
0.4	4.12	1630	29
0.5	6.24	1880	36
0.6	8.72	2120	42
0.7	11.5	2320	48
0.8	14.6	2490	53
0.9	17.9	2630	57
1.0	21.4	2740	61

(b) The decay of Pb corrosion product activity following one year operation at 1 mA and for a corrosion rate corresponding to 0.1 cm/year.

	Decay Time (days) →						
	0.0	0.1	10.0	30.0	100.0	365.0	730.0
Curies	2740	2720	2240	1890	1260	466	225
'Burden'	61	61	55	49	35	20	17

is to be expected in the irradiated regions from radiolysis: there will be an experimental programme to measure the corrosion rates (with beam) together with the effect of water processing. It is planned to clad the Pb-shot with Sn: with appropriate circuit layout and provision of suitable shielding the problem would not seem to be too serious. The activation contribution of corrosion products would appear to make a rather insanitary water-cooling system more so, but not by a huge factor.

Afterheat. The peak decay power density immediately after beam turn-off following operation at 25  $\mu\text{A}/\text{cm}^2$  is  $\leq 100$  mW/g. This would melt the peak-rated Pb-shot in about 10 mins (starting from 40 °C) if the Pb was completely thermally isolated. The corresponding surface power density is about 100 mW/cm<sup>2</sup> (which would be balanced by black-body radiation at 600 k for a surface emissivity of  $\geq 0.2$ ). After about 10 days cool-down period (a typical time delay before a target change) the corresponding figures are 10 mW/g, 100 mins and 9 mW/cm<sup>2</sup>. It is not yet clear how high the time-averaged current density will be over a year's operating period.

The vertical geometry implies that a complete window break will make it rather inconvenient to keep coolant in contact with the Pb. The adoption of a two-element window will alleviate this if the probability of both window-elements breaking simultaneously is significantly lower than that for one and a means of detecting the failure of either one is provided.

Radiation Damage: A major uncertainty will be the life-limit of the beam window (which most likely will come from radiation damage although thermal cycling has to be considered also). The choice of aluminium has a major advantage that we do have some practical experience. The BMA-window here at PSI (constructed from Alusuisse type AC-100 aluminium) passes 16  $\mu\text{A}$  of 590 MeV protons with a beam diameter of less than 5 mm (i.e. a current density in the region of 80  $\mu\text{A}/\text{cm}^2$ ). To date, these windows have not failed in operation (but are regularly changed after about 40,000  $\mu\text{A} \cdot \text{hrs}$  operation). Two have been taken out, the first after about 50,000 and the second after 30,000  $\mu\text{A} \cdot \text{hrs}$  operation, for examination: neither window showed visible signs of damage.

To complete a first conceptual design study, the following points have to be worked on:-

1. Optimization of the pebble-bed: confirmation of the flow-diverter concept, choice of shot-size (the size of the Pb-shot should be increased in the lower power density regions to (i) reduce the pressure drop and (ii) reduce the surface area presented to the  $D_2O$  for corrosion).
2. A concept for the neutronic sensitive region above 50 cm. We would like to begin the shielding as early as possible but power levels are still high enough in this region to require careful cooling design.
3. Shielding: Target handling is designed to involve "hands-on" tasks in preparing the target for removal. Steel shielding will be introduced after 100 cm but has to incorporate all the service connections and will also require cooling at the bottom end.
4. A complete handling concept for the target system - uncoupling the coolant circuit - transfer vessel - provision of cooling for after-heat etc.
5. Design of the external parts of the main cooling loop, including provision of water processing and adequate shielding against accumulated activation.

## References

- [1] F. Atchison, "The Neutronic Performance of Solid Target Alternatives for SINQ"  
- Contribution to these proceedings.
- [2] M. Dubs and J. Ulrich, "Design Considerations for the SINQ Target window"  
- Contribution to these proceedings.
- [3] S. Whitaker, "Fundamental Principles of Heat Transfer", Pergamon Press (1977)
- [4] E. Achenbach, Chem. Ing. Tech. 54, 66 (1982)
- [5] E.U. Schlünder, "Wärme und Stoffübertragung zwischen durchströmten Schüttungen",  
Chemie-Ing 38, 967 (1966)
- [6] G. Heidenreich, "Preliminary thermal and stress analysis for the SINQ window"  
- Contribution to these proceedings.
- [7] ANSYS, Swanson Analysis Systems Inc., Houston, PA 15324, USA